Supplementary Information

Supplementary Figure Legends

Figure S1. (A) Histograms represent median fluorescence intensity of surface immunoglobulin expression in LCLs determined by flow cytometry. **(B)** Correlation matrix (Pearson's correlation coefficient) between biological replicates for the LCL GPome, based on SILAC fold change values for all quantified p-sites. H: heavy (BCR-stimulated LMP2A-KO), M: medium (EBV-WT), L: light (LMP2A-KO). **(C-D)** Western blot analysis of total tyrosine phosphorylation (C) and selective BCR downstream effectors (D) in 5-minute BCR-stimulated and unstimulated LCLs. **(E)** Pathway enrichment analysis (Reactome terms) for proteins differentially phosphorylated (Up: significantly increased, Down: significantly decreased; Benjamini-Hochberg adjusted p-value < 0.001 and absolute $\log_2$ fold change ≥ 1) in the GPome of EBV-WT (blue) or BCR-stimulated LMP2A-KO (orange) LCLs relative to LMP2A-KO cells.

Figure S2. (A) Scatter plot of log2 SILAC ratios for the GPome from BCR-stimulated or LMP2A-positive MYC-expressing mouse B cells, normalized to unstimulated MYC-expressing mouse B cells. The Spearman's rank correlation coefficient (r) is shown. Orange and blue dots indicate significantly concordantly and discordantly regulated p-sites, respectively, and selected hits are labeled. **(B)** Same as (A), for the pYome. **(C)** Pathway enrichment analysis (Reactome terms) for proteins differentially phosphorylated (Up: significantly increased, Down: significantly decreased) in the GPome of LMP2A-positive MYC-expressing mouse B cells, normalized to unstimulated MYC-expressing mouse B cells. Pathways that were also significantly enriched in LCLs are indicated in boldface.

Figure S3. (A) The network topology of genes encoding proteins related to BCR signaling is shown. For each protein, significant changes in phosphorylation in the LCL pYome are color-coded as indicated (left icon: EBV-WT; right icon: BCR-stimulation LMP2A-KO). Proteins that do not exhibit concordantly increased or decreased phosphorylation across all p-sites are referred to as 'mixed'.

Figure S4. (A) Principal component analysis of EBV-WT, LMP2A-KO and BCR-stimulated LMP2A-KO LCL gene expression. Genes with zero counts across all samples were excluded from the analysis. **(B)** Hierarchical clustering of the top 50 differentially expressed genes (adjusted p-value ≤ 10−5, likelihood ratio test). **(C)** Pathway enrichment analysis (Reactome terms) for genes

that were differentially expressed in the indicated conditions.

Figure S5. (A) Validation of indicated pro- and anti-apoptotic protein expression in LCLs by Western blot analysis.

Dataset Legends

Dataset S1. Quantified p-sites from the global phosphoproteome (GPome) in human LCLs, and significantly differentially phosphorylated p-sites.

Dataset S2. Quantified p-sites from the tyrosine phosphoproteome (pYome) in human LCLs, and significantly differentially phosphorylated p-sites.

Dataset S3. Quantified p-sites from the global phosphoproteome (GPome) in Myc-expressing transgenic mouse cells, and significantly differentially phosphorylated p-sites.

Dataset S4. Quantified p-sites from the tyrosine phosphoproteome (pYome) in Myc-expressing transgenic mouse cells, and significantly differentially phosphorylated p-sites.

Dataset S5. Differentially expressed genes from RNA-seq profiling of human LCLs.

Dataset S6. Enriched gene signatures from gene signature enrichment analysis based on quantified gene expression.

Dataset S7. Quantified proteins from total proteome analysis of human LCLs, and differentially expressed proteins.

Figure S1

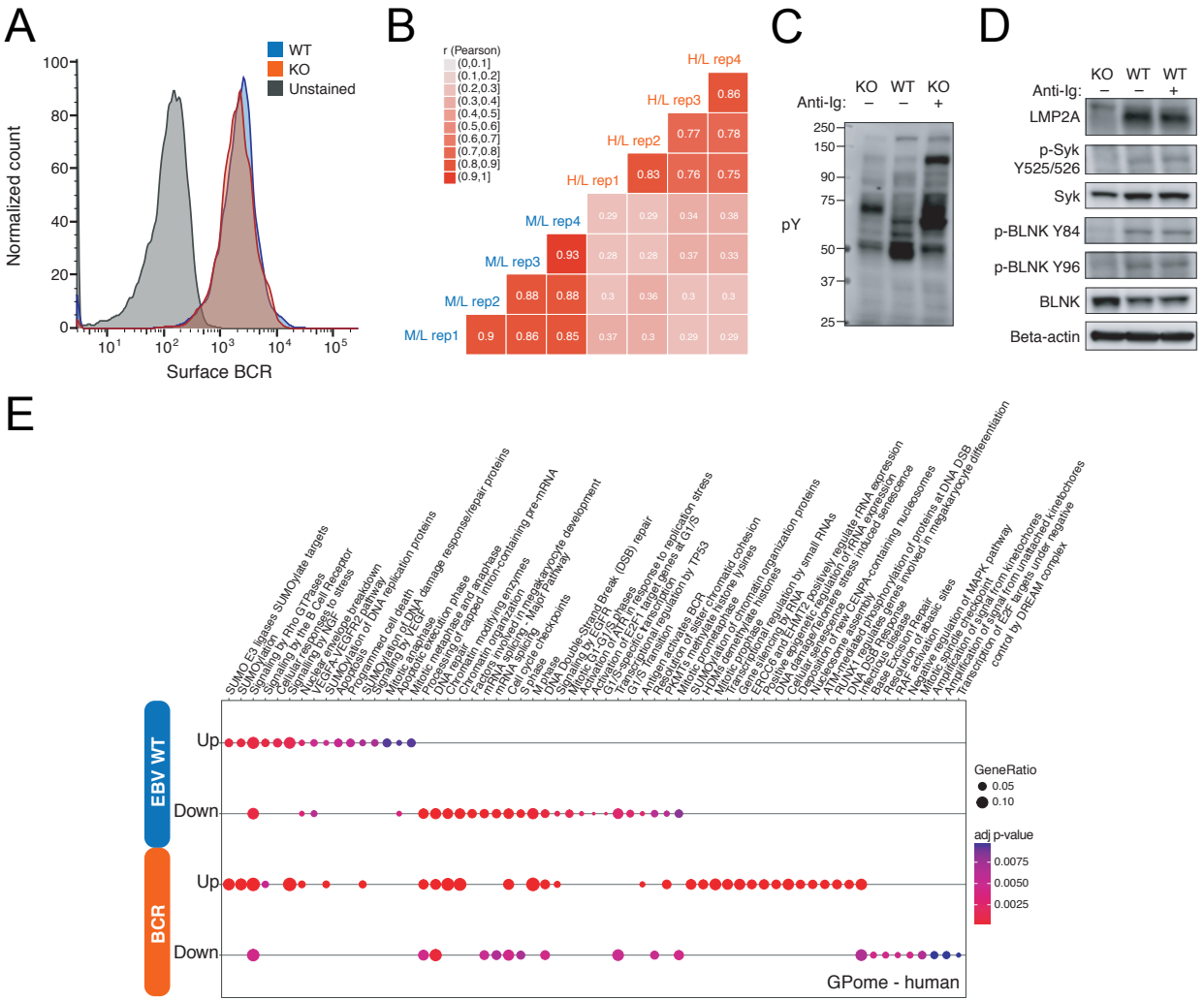
A
WT
KO
Unstained
Normalized count
Surface BCR
B
r (Pearson)
(0,0.1]
(0.1,0.2]
(0.2,0.3]
(0.3,0.4]
(0.4,0.5]
(0.5,0.6]
(0.6,0.7]
(0.7,0.8]
(0.8,0.9]
(0.9,1]
H/L rep4
H/L rep3
H/L rep2
H/L rep1
M/L rep4
M/L rep3
M/L rep2
M/L rep1
C
KO WT KO
Anti-Ig: – – +
pY
D
KO WT WT
Anti-Ig: – – +
LMP2A
p-Syk Y525/526
Syk
p-BLNK Y84
p-BLNK Y96
BLNK
Beta-actin
E
EBV WT
BCR
Up
Down
GeneRatio
adj p-value
GPome - human

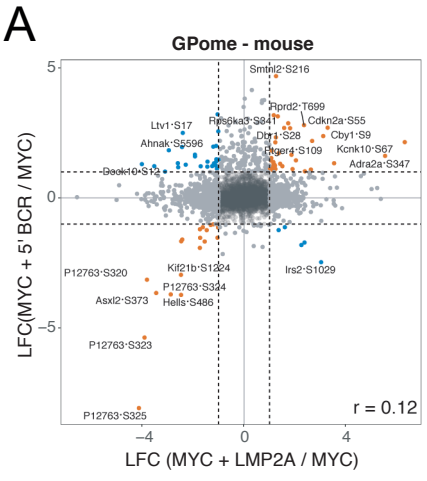
A
GPome - mouse
Smtnl2·S216
Hprd2·T699
Rps6ka3·S841
Cdkn2a·S55
Ltv1·S17
Dbn1·S28
Cby1·S9
Ahnak·S5596
Rgcc4·S109
Kcnk10·S67
Adra2a·S347
Bcok10·S12
Kif21b·S1224
P12763·S320
Irs2·S1029
P12763·S324
Asxl2·S373
Hells·S486
P12763·S323
P12763·S325
r = 0.12
LFC(MYC + 5' BCR / MYC)
LFC (MYC + LMP2A / MYC)

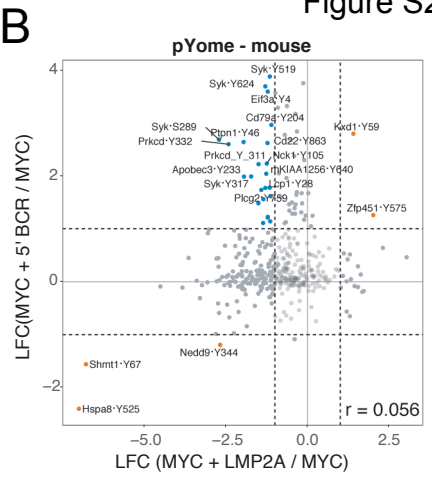
B
pYome - mouse
Syk·Y519
Syk·Y624
Eif3g·Y4
Cd79a·Y204
Kxd1·Y59
Syk·S289
Ptpn1·Y46
Prkcd·Y332
Cd22·Y863
Prkcd_Y_311
Nck1·Y105
Apobec3·Y233
rhKIAA1256·Y640
Syk·Y317
Lcp1·Y28
Plcg2·Y759
Zfp451·Y575
Nedd9·Y344
Shmt1·Y67
Hspa8·Y525
r = 0.056
LFC(MYC + 5' BCR / MYC)
LFC (MYC + LMP2A / MYC)

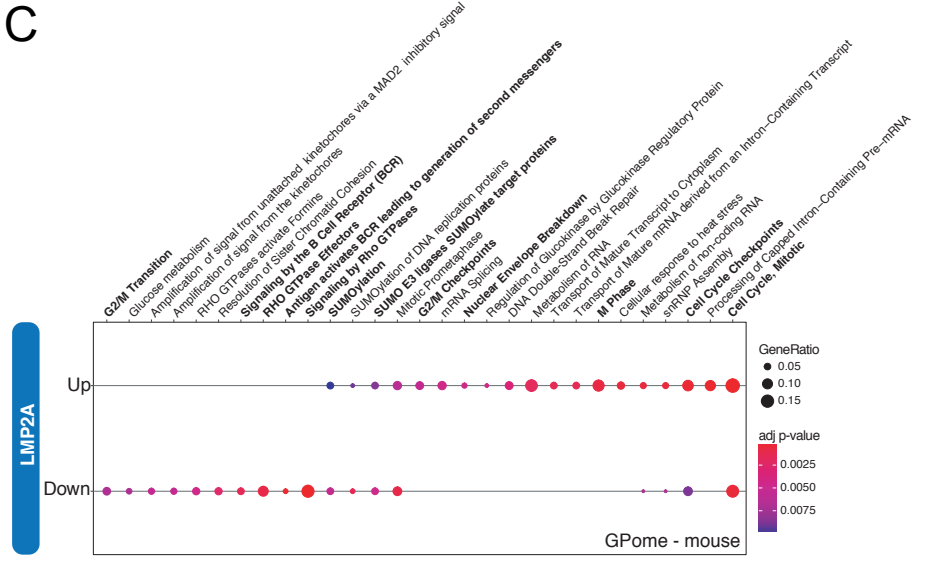
C
G2/M Transition
Glucose metabolism
Amplification of signal from unattached kinetochores via a MAD2 inhibitory signal
Amplification of signal from the kinetochores
RHO GTPases activate Formins
Resolution of Sister Chromatid Cohesion
Signaling by the B Cell Receptor (BCR)
RHO GTPase Effectors
Antigen activates BCR leading to generation of second messengers
Signaling by Rho GTPases
SUMOylation
SUMO E3 ligases SUMOylate target proteins
SUMOylation of DNA replication proteins
G2/M Checkpoints
Mitotic Prometaphase
Nuclear Envelope Breakdown
mRNA Splicing
Regulation of Glucokinase by Glucokinase Regulatory Protein
DNA Double-Strand Break Repair
Metabolism of RNA
Transport of Mature Transcript to Cytoplasm
M Phase
Transport of Mature mRNA derived from an Intron-Containing Transcript
Cellular response to heat stress
Metabolism of non-coding RNA
snRNP Assembly
Cell Cycle Checkpoints
Processing of Capped Intron-Containing Pre-mRNA
Cell Cycle, Mitotic
LMP2A
Up
Down
GeneRatio
0.05
0.10
0.15
adj p-value
0.0025
0.0050
0.0075
GPome - mouse

A

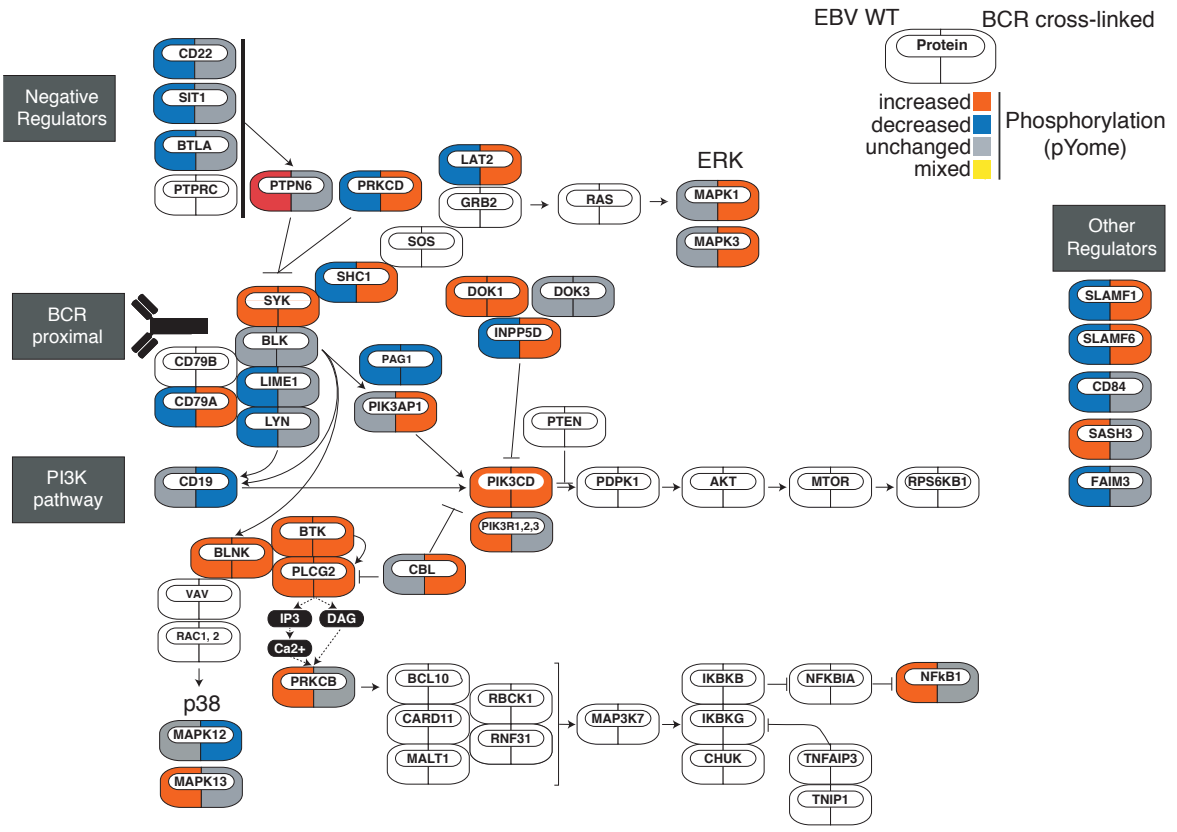
EBV WT
BCR cross-linked
Protein
increased
decreased
unchanged
mixed
Phosphorylation (pYome)
Negative Regulators
CD22
SIT1
BTLA
PTPRC
PTPN6
PRKCD
LAT2
GRB2
RAS
ERK
MAPK1
MAPK3
SOS
SHC1
BCR proximal
SYK
BLK
LIME1
LYN
CD79B
CD79A
DOK1
DOK3
INPP5D
PAG1
PIK3AP1
PTEN
PI3K pathway
CD19
PIK3CD
PDPK1
AKT
MTOR
RPS6KB1
PIK3R1,2,3
BTK
BLNK
PLCG2
CBL
VAV
RAC1, 2
IP3
DAG
Ca2+
PRKCB
p38
MAPK12
MAPK13
BCL10
CARD11
MALT1
RBCK1
RNF31
MAP3K7
IKBKB
IKBKG
CHUK
NFKBIA
NFKB1
TNFAIP3
TNIP1
Other Regulators
SLAMF1
SLAMF6
CD84
SASH3
FAIM3

Figure S4

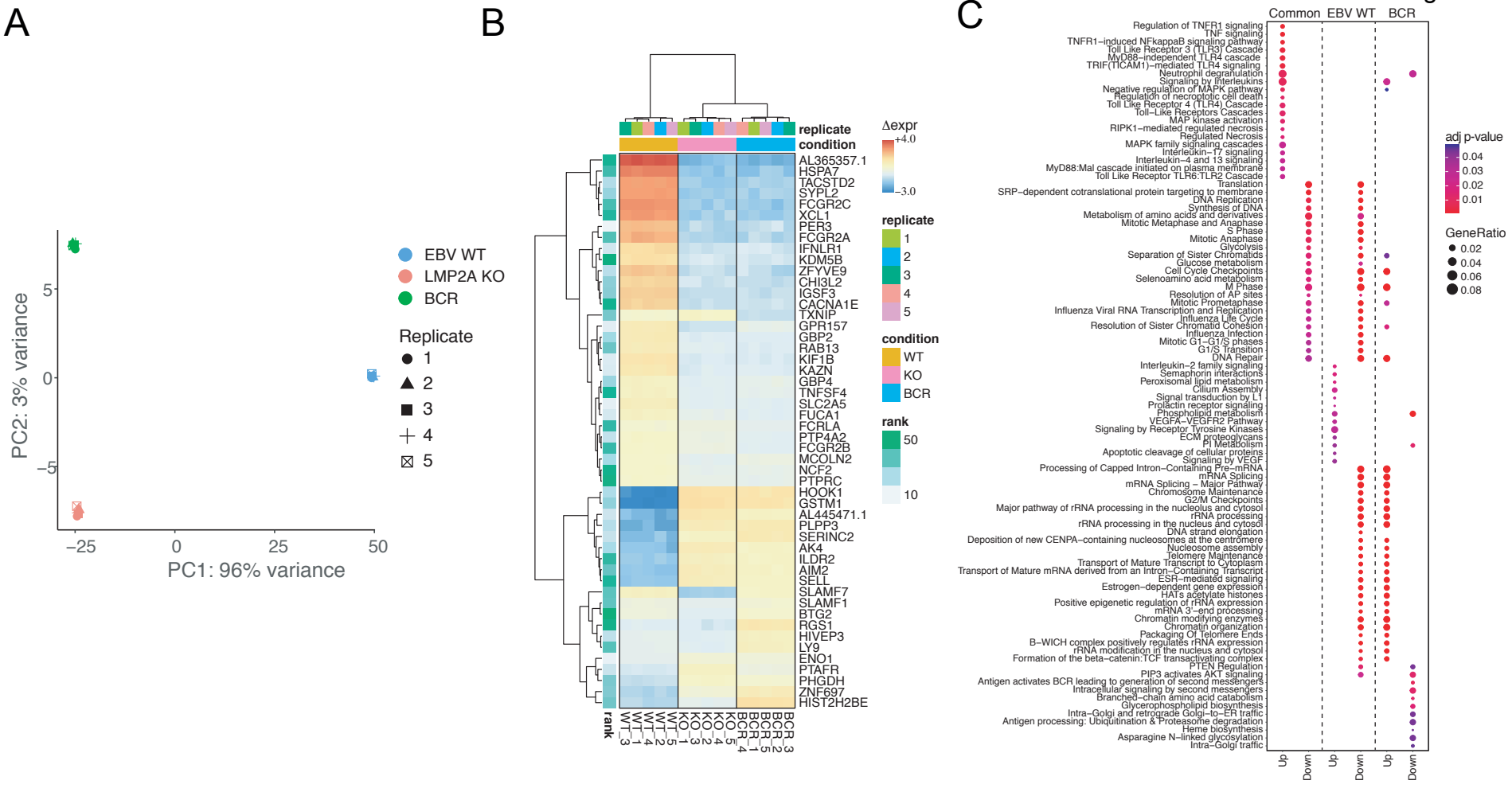
A
PC2: 3% variance
PC1: 96% variance
EBV WT
LMP2A KO
BCR
Replicate
1
2
3
4
5
B
replicate
condition
Δexpr
+4.0
−3.0
replicate
condition
WT
KO
BCR
rank
50
10
AL365357.1
HSPA7
TACSTD2
SYPL2
FCGR2C
XCL1
PER3
FCGR2A
IFNLR1
KDM5B
ZFYVE9
CHI3L2
IGSF3
CACNA1E
TXNIP
GPR157
GBP2
RAB13
KIF1B
KAZN
GBP4
TNFSF4
SLC2A5
FUCA1
FCRLA
PTP4A2
FCGR2B
MCOLN2
NCF2
PTPRC
HOOK1
GSTM1
AL445471.1
PLPP3
SERINC2
AK4
ILDR2
AIM2
SELL
SLAMF7
SLAMF1
BTG2
RGS1
HIVEP3
LY9
ENO1
PTAFR
PHGDH
ZNF697
HIST2H2BE
C
Common
EBV WT
BCR
Regulation of TNFR1 signaling
TNF signaling
TNFR1−induced NFkappaB signaling pathway
Toll Like Receptor 3 (TLR3) Cascade
MyD88−independent TLR4 cascade
TRIF(TICAM1)−mediated TLR4 signaling
Neutrophil degranulation
Signaling by Interleukins
Negative regulation of MAPK pathway
Regulation of necroptotic cell death
Toll Like Receptor 4 (TLR4) Cascade
Toll−Like Receptors Cascades
MAP kinase activation
RIPK1−mediated regulated necrosis
Regulated Necrosis
MAPK family signaling cascades
Interleukin−17 signaling
Interleukin−4 and 13 signaling
MyD88:Mal cascade initiated on plasma membrane
Toll Like Receptor TLR6:TLR2 Cascade
Translation
SRP−dependent cotranslational protein targeting to membrane
DNA Replication
Synthesis of DNA
Metabolism of amino acids and derivatives
Mitotic Metaphase and Anaphase
S Phase
Mitotic Anaphase
Glycolysis
Separation of Sister Chromatids
Glucose metabolism
Cell Cycle Checkpoints
Selenoamino acid metabolism
M Phase
Resolution of AP sites
Mitotic Prometaphase
Influenza Viral RNA Transcription and Replication
Influenza Life Cycle
Resolution of Sister Chromatid Cohesion
Influenza Infection
Mitotic G1−G1/S phases
G1/S Transition
DNA Repair
Interleukin−2 family signaling
Semaphorin interactions
Peroxisomal lipid metabolism
Cilium Assembly
Signal transduction by L1
Prolactin receptor signaling
Phospholipid metabolism
VEGFA−VEGFR2 Pathway
Signaling by Receptor Tyrosine Kinases
ECM proteoglycans
PI Metabolism
Apoptotic cleavage of cellular proteins
Signaling by VEGF
Processing of Capped Intron−Containing Pre−mRNA
mRNA Splicing
mRNA Splicing − Major Pathway
Chromosome Maintenance
G2/M Checkpoints
Major pathway of rRNA processing in the nucleolus and cytosol
rRNA processing
rRNA processing in the nucleus and cytosol
DNA strand elongation
Deposition of new CENPA−containing nucleosomes at the centromere
Nucleosome assembly
Telomere Maintenance
Transport of Mature Transcript to Cytoplasm
Transport of Mature mRNA derived from an Intron−Containing Transcript
ESR−mediated signaling
Estrogen−dependent gene expression
HATs acetylate histones
Positive epigenetic regulation of rRNA expression
mRNA 3'−end processing
Chromatin modifying enzymes
Chromatin organization
Packaging Of Telomere Ends
B−WICH complex positively regulates rRNA expression
rRNA modification in the nucleus and cytosol
Formation of the beta−catenin:TCF transactivating complex
PTEN Regulation
PIP3 activates AKT signaling
Antigen activates BCR leading to generation of second messengers
Intracellular signaling by second messengers
Branched−chain amino acid catabolism
Glycerophospholipid biosynthesis
Intra−Golgi and retrograde Golgi−to−ER traffic
Antigen processing: Ubiquitination & Proteasome degradation
Heme biosynthesis
Asparagine N−linked glycosylation
Intra−Golgi traffic
Up
Down
adj p-value
0.04
0.03
0.02
0.01
GeneRatio
0.02
0.04
0.06
0.08

Figure S5

A

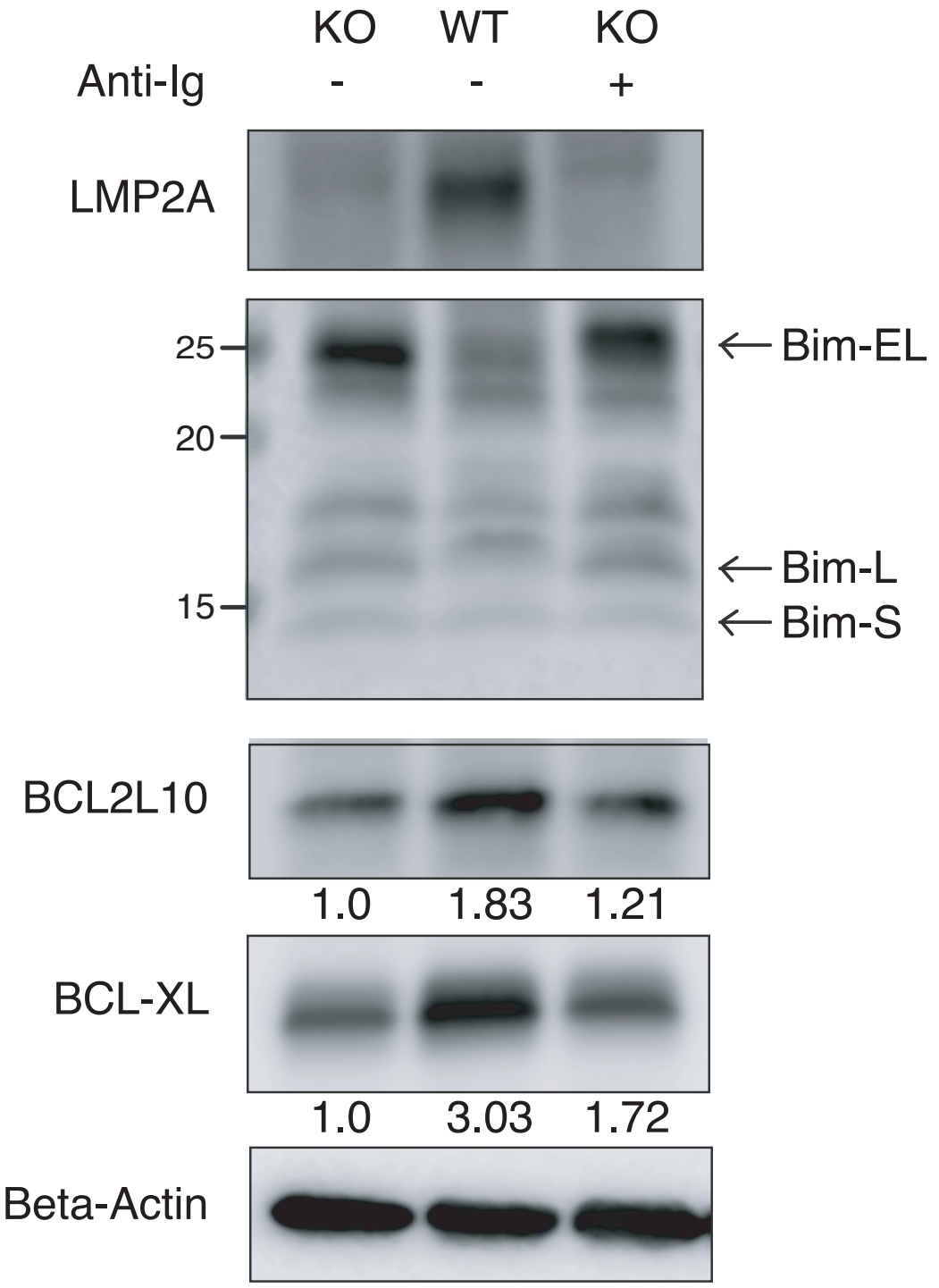
KO
WT
KO
Anti-Ig
-
-
+
LMP2A
25
20
15
← Bim-EL
← Bim-L
← Bim-S
BCL2L10
1.0
1.83
1.21
BCL-XL
1.0
3.03
1.72
Beta-Actin